JOURNAL OF THE MECHANICAL BEHAVIOR OF BIOMEDICAL MATERIALS 42 (2015) 54–66

Available online at www.sciencedirect.com

ScienceDirect

www.elsevier.com/locate/jmbbm

Research Paper

Compressive strength of elderly vertebrae is reduced by disc degeneration and additional flexion ☆

Ghislain Maquer[a], *Jakob Schwiedrzik*[a], *Gerd Huber*[b], *Michael M. Morlock*[b], *Philippe K. Zysset*[a,*]

[a]*Institute of Surgical Technology and Biomechanics, University of Bern, Stauffacherstrasse 78, CH-3014 Bern, Switzerland*

[b]*Institute of Biomechanics, Hamburg University of Technology, Denickestraße 15, 21073 Hamburg, Germany*

ARTICLE INFO

Article history:
Received 10 June 2014
Received in revised form
29 October 2014
Accepted 31 October 2014
Available online 11 November 2014

Keywords:
Finite element analysis
Vertebral strength
Osteoporosis
Intervertebral disc degeneration
Calibration

ABSTRACT

Computer tomography (CT)-based finite element (FE) models assess vertebral strength better than dual energy X-ray absorptiometry. Osteoporotic vertebrae are usually loaded via degenerated intervertebral discs (IVD) and potentially at higher risk under forward bending, but the influences of the IVD and loading conditions are generally overlooked. Accordingly, magnetic resonance imaging was performed on 14 lumbar discs to generate FE models for the healthiest and most degenerated specimens. Compression, torsion, bending, flexion and extension conducted experimentally were used to calibrate both models. They were combined with CT-based FE models of 12 lumbar vertebral bodies to evaluate the effect of disc degeneration compared to a loading via endplates embedded in a stiff resin, the usual experimental paradigm. Compression and lifting were simulated, load and damage pattern were evaluated at failure. Adding flexion to the compression (lifting) and higher disc degeneration reduces the failure load (8–14%, 5–7%) and increases damage in the vertebrae. Under both loading scenarios, decreasing the disc height slightly increases the failure load; embedding and degenerated IVD provides respectively the highest and lowest failure load. Embedded vertebrae are more brittle, but failure loads induced via IVDs correlate highly with vertebral strength. In conclusion, osteoporotic vertebrae with degenerated IVDs are consistently weaker—especially under lifting, but clinical assessment of their strength is possible via FE analysis without extensive disc modelling, by extrapolating measures from the embedded situation.

☆Grants: Swiss National Science Foundation (SNF), grant no 325230_147153, German Federal Ministry of Education and Research (BMBF), grant no 01EC1005.

*Corresponding author. Tel.: +41 31 631 59 25; fax: +41 31 631 59 60.
E-mail address: philippe.zysset@istb.unibe.ch (P.K. Zysset).

http://dx.doi.org/10.1016/j.jmbbm.2014.10.016
1751-6161/

1. Introduction

With nearly half a million cases a year in Europe, osteoporotic vertebral fractures are a widespread condition with tremendous costs and morbidity (Johnell and Kanis, 2005). Osteoporosis is characterized by bone loss and impaired bone morphology. Fracture occurs when the load on a bone is larger than its overload or fatigue strength. Strength and mineral density (BMD) are therefore highly related and non-invasive radiographic techniques were developed to evaluate the fracture risk. Yet, as Dual energy X-ray absorptiometry (DXA), the clinical surrogate for strength, accounts neither for morphology, nor for local variation of bone density (Griffith and Genant, 2008) or loading conditions, it explains less than 70% of the strength variability (Lochmüller et al., 2002). Quantitative computer tomography (QCT)-based finite element (FE) models of the vertebral body are used in clinical trials (Keaveny et al., 2007; Graeff et al., 2009, 2013; Chevalier et al., 2010; Farahmand et al., 2013; Glüer et al., 2013; Kopperdahl et al., 2014) but not yet for diagnosis, although their strength predictions are more accurate than densitometric methods (Crawford et al., 2003; Dall'Ara et al., 2012). To ensure uniform compression of the bone and overlook the degenerative states of elderly intervertebral discs (IVD) (Keller et al., 1993), the endplates are trimmed (vertebral sections) or embedded in a stiff resin (polymethylmethacrylate, PMMA). Both methods are reproducible, validated (Dall'ara et al., 2010; Chevalier et al., 2008) and highly correlated (Maquer et al., 2012) but common endplate failure cannot be replicated (Nekkanty et al., 2010; Maquer et al., 2014a). Compression overestimates the strength of osteoporotic vertebrae that are weaker under forward bending due to an altered trabecular structure (Homminga et al., 2004). The load distribution on the endplate is affected by alterations of the IVD due to degenerative processes (Adams and Roughley, 2006). It seems relevant to account for the IVD in future FE analyses (Eswaran et al., 2007) but there is a lack of reliable degeneration-specific model (Lu et al., 2014). Most models are based on prior literature, with generic shapes and material properties (Fagan et al., 2002; Weisse et al., 2012, Park et al., 2013) without considering the inter-individual and experimental variability (Jones and Wilcox, 2008). Addressing these limitations, healthy and degenerated IVD models calibrated against in vitro tests and endplate embedding were used to load vertebral bodies under uniaxial compression and lifting. The hypothesis of this study is that disc degeneration and forward flexion weaken osteoporotic vertebrae; its aim is to evaluate the influence of the loading conditions on the predicted vertebral failure load and damage distribution and to determine whether FE strength predictions would benefit from a better modelling of the IVD.

1.1. *Specimen-specific modelling of the intervertebral disc*

1.1.1. *Preparation and selection of the specimens*

Fourteen spinal units (T12–L1, L2–L3, L4–L5) were extracted from 6 human lumbar spines and frozen (−20 °C) after approval of the Ethics Committee of the Medical University of Vienna. The specimens were thawed at room temperature (20 °C) 24 h before neural arch and most soft tissues, but IVDs were removed. The free caudal and cranial endplates were embedded in a 10 mm-thick layer PMMA (Fig. 1). MRI imaging was performed on the specimens placed in a water-filled container (0.9% saline) to avoid drying and ensure loading of the RF coil. T_1 weighted (T_R=999 ms, T_E=13 ms, 0.3 mm in-plane, 0.8 mm out-of-plane resolution) and quantitative T_2 images (T_R=3650 ms, first echo: 12.5 ms, last echo: 275 ms, steps: 12.5 ms, 0.5 mm resolution) were acquired via a 3 T system (Verio, Siemens Healthcare, Germany). The non-invasive evaluation of the specimens' degeneration was done independently by 2 experts based on their mid-sagittal appearance (Thompson et al., 1990), transverse T_2-maps (Watanabe et al., 2007) and Benneker et al. (2005) score, validated against biochemical markers of degeneration. The healthiest (Grade I) and most degenerated (Grade IV) spinal units were kept for testing. Please refer to Maquer et al. (2014b) for more details.

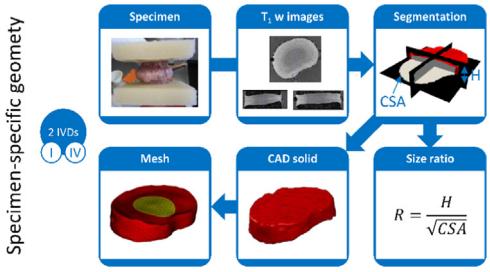

Fig. 1 – MRI-based FE meshes were generated from T_1 weighted images of the healthy (grade I) and degenerated (grade IV) specimens. Both discs were segmented. Size ratio (*R*) was computed for each specimen from height (*H*) and cross-sectional area (CSA) established from the segmented volume. Central nucleus (yellow) and the surrounding annulus (red) were partitioned and the volumes meshed. The meshing pipeline was adapted from Ribeiro et al. (2009). (For interpretation of the references to color in this figure legend, the reader is referred to the web version of this article.)

1.1.2. *MRI-based disc geometry*

MRI data was also used mesh both specimens and determine their dimensions (Fig. 1). The discs were semi-automatically segmented from the T_{1w} images via ITKSnap (Yushkevich et al., 2006). Volume (*V*), cross-sectional area (CSA), average disc height (*H*) and size ratio (*R*) were determined (Eq. (1)).

$$CSA = \sum_{i}^{N} CSA_i \quad V = \sum_{i}^{M} V_i \quad H = \frac{V}{CSA} \quad R = \frac{H}{\sqrt{CSA}} \tag{1}$$

V was evaluated by summing the volume of the disc's voxels V_i (*M* voxels per disc) and CSA was computed by adding the CSA_i of the disc's voxels (*N* voxels per cross-section). A size ratio was obtained for the healthy (R_I) and degenerated IVDs (R_{IV}). The segmented volumes were imported in Solidworks as.stl meshes via ScanTo3D (Dassault Systèmes, France) and 2 solids were generated by fitting surface patches onto the smoothened meshes. Partition between *NP* and *AF* (42% volume ratio, Goto et al., 2002; Moramarco et al., 2010; Wang et al., 2013) was performed on both solids that were